

Terahertz surface impedance of epitaxial MgB₂ thin film

B. B. Jin

Institut für Schichten und Grenzflächen (ISG) and cni-Center of Nanoelectronic Systems for Information Technology, Forschungszentrum Jülich, 52425 Jülich, Germany

P. Kuzel and F. Kadlec

Institute of Physics, Academy of Sciences of the Czech Republic, Na Slovance 2, 182 21 Prague 8, Czech Republic

T. Dahm

Universität Tübingen, Institut für Theoretische Physik, Auf der Morgenstelle 14, 72076 Tübingen, Germany

J. M. Redwing

The Department of Material Science and Engineering, The Pennsylvania State University, University Park, Pennsylvania 16802

A. V. Pogrebnikov and X. X. Xi

The Department of Physics and The Department of Material Science and Engineering, The Pennsylvania State University, University Park, Pennsylvania 16802

N. Klein

Institut für Schichten und Grenzflächen (ISG) and cni-Center of Nanoelectronic Systems for Information Technology, Forschungszentrum Jülich, 52425 Jülich, Germany

(Received 28 March 2005; accepted 20 July 2005; published online 22 August 2005)

We report on terahertz (THz) surface impedance measurement of an epitaxial MgB₂ thin film using time domain THz spectroscopy. We show that the surface resistance of the MgB₂ film is much lower than that of YBa₂Cu₃O_{7- δ} and copper in the THz range. A linear dependence of the surface reactance on frequency is observed, yielding a penetration depth of about 100 nm at low temperatures. The measurements agree qualitatively with calculations based on impurity scattering in the Born limit. Our results clearly indicate that MgB₂ thin films have a great potential for THz electronic applications. © 2005 American Institute of Physics. [DOI: [10.1063/1.2034107](https://doi.org/10.1063/1.2034107)]

Terahertz (THz) and infrared spectroscopic measurements on superconductors play an important role in understanding their superconducting properties.¹⁻³ These measurements probe the frequency dependence of the complex conductivity over a wide frequency range below and above the energy gap, which yields important information on the properties of low-energy excitations, scattering rate and coherence effect. In addition, these measurements are also essential for THz superconducting electronic devices.⁴ It is well known that superconducting electronic devices have demonstrated specific advantages at sub-mm and THz frequencies. Especially, for frequencies beyond 1 THz, superconducting hot electron bolometers (HEBs) appear to be the only option for low noise heterodyne mixing elements. The design, simulation, and improvement of THz superconducting electronic devices rely on the understanding of the superconducting film properties at THz frequencies.

The discovery of superconductivity in MgB₂ has attracted much research effort because MgB₂ may be the clearest example of two-gap superconductivity with a high critical temperature (T_c) of 39 K and a simple binary chemical composition.^{5,6} THz and infrared spectroscopic measurements were carried out soon after its discovery.⁷⁻⁹ The results clearly showed the existence of a small energy gap caused by the π -bands. In this Letter we present our investigations on an epitaxial thin film using time-domain THz spectroscopy (TDTS). The THz and infrared spectroscopies are commonly performed in transmission or reflective modes. The transmission measurements applied to superconductors usually offer higher accuracy than the reflection measurement because the sample reflectance is close to unity for energies below the

gap. In the transmission measurement, a very thin film with high quality is needed to achieve higher transmitted power for improving signal-to-noise ratio, and to avoid extrinsic effects, such as the increased carrier scattering due to a high density of defects. In this work, the MgB₂ thin film was deposited by a hybrid physical-chemical vapor deposition technique (HPCVD), which produces epitaxial thin films with small thickness and high T_c .¹⁰ Theoretical calculations of the complex conductivity σ based on impurity scattering in the Born limit within a two band superconductor are presented. The surface impedance $Z_s = R_s + jX_s$ is derived by taking $Z_s = (j\omega\mu/\sigma)^{1/2}$, and then compared with our experimental results. Here, R_s , X_s , ω , and μ are surface resistance, surface reactance, angular frequency, and free-space permeability, respectively.

The details of HPCVD deposition of epitaxial MgB₂ thin films can be found in Ref. 10. The film used in this work was deposited on sapphire substrate and has a nominal thickness of 100 nm with a T_c of 39.1 K and a sharp transition width of less than 0.3 K. High-resolution transmission electron microscopy showed that for the HPCVD MgB₂ films on sapphire substrate, there is a 30–40 nm thick interface layer between the Al₂O₃ substrate and the MgB₂ film where MgO regions exist.¹⁰ For the analysis of the surface impedance of this particular film we therefore assumed that the actual thickness of the superconducting layer to be 62 nm: For this value the best agreement between the dc resistivity determined from microwave and dc measurements was achieved.

Our TDTS measurement utilizes ultrashort broadband THz pulses generated and detected, respectively, by optical rectification and electro-optic sampling in 1 mm thick [110]-

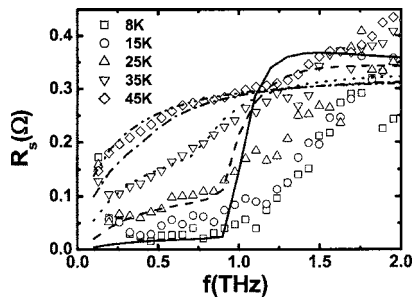


FIG. 1. The frequency dependence of surface resistance R_s at 8 K (squares), 15 K (circles), 25 K (upper triangles), 35 K (down triangles), and 45 K (diamonds). The lines represent the calculations at the same set of temperatures, which are based on the model described in the text.

oriented ZnTe single crystals. This arrangement enables us to measure the amplitude as well as the phase shift of the transmitted THz wave. The complex conductivity of the MgB_2 thin film can be calculated without any model assumption and without a Kramers–Kronig transformation. The details are described in Refs. 11–14. In our measurements, the typical value of the THz power transmission coefficient at low temperatures ($T < 40$ K) is about 10^{-4} . Note also that the THz conductivity of our sample is by more than one order of magnitude higher than that reported in Ref. 7.

Figures 1 and 2 show the frequency dependence of surface resistance R_s and surface reactance X_s , respectively at 8 K, 15 K, 25 K, 35 K, and 45 K. The lines represent the theoretical calculations, which will be discussed later. The frequency dependence of R_s , as shown in Fig. 1, display a two-stage behavior. At low frequencies it increases slowly with frequency, and then with a steeper slope at high frequencies. This two-stage behavior is more pronounced when the temperature is decreased. This agrees qualitatively with the theoretical prediction that there is a jump in R_s when the probing frequency (the photon energy) equals two times the (small) energy gap value [about 2 meV at 0 K (Ref. 6)]. The magnitude of the jump becomes larger when the temperature decreases.¹ For X_s , a linear dependence could be observed in Fig. 2 for all temperatures. The plots are shifted vertically by 0.2Ω relative to each other for clarity. Since the surface reactance is given by $X_s = \omega \mu \lambda$, the linear dependence indicates a frequency independence of the penetration depth λ over the whole frequency range. We find that λ at 8 K is 104 nm.

With regards to applications in THz electronics, we compare the R_s values of MgB_2 thin film with $\text{YBa}_2\text{Cu}_3\text{O}_{7-\delta}$ (YBCO) and copper. YBCO is a potential candidate for THz

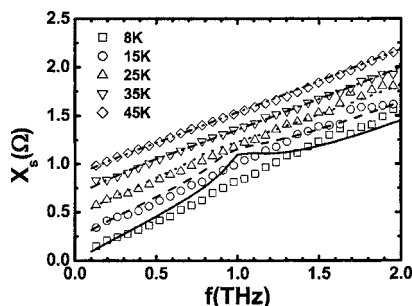


FIG. 2. Frequency dependence of the surface reactance X_s at 8 K (squares), 15 K (circles), 25 K (upper triangles), 35 K (down triangles), and 45 K (diamonds). The lines represent the calculations at the same set of temperatures, which are based on the model described in the text. Note that the symbols and lines are vertically shifted by 0.2Ω relative to each other.

TABLE I. Residual surface resistance R_{res} of YBCO (Refs. 13 and 14), surface resistances R_s of MgB_2 at 8 K and 15 K at 0.45 THz, 1 THz, and 2 THz.

f (THz)	0.45	1	2
R_{res} (Ω) (YBCO)	0.22	0.3	1
R_s (Ω) (MgB_2 at 8 K)	0.027	0.052	0.27
R_s (Ω) (MgB_2 at 15 K)	0.03	0.096	0.35

application because of its high T_c and large energy gap value.¹⁵ Copper has low surface resistances at low temperatures and THz frequencies.⁴ Table I lists the R_s of MgB_2 and the residual surface resistance $R_{\text{res}}[R_s(T \rightarrow 0)]$ of YBCO at 8 K and 15 K, at a frequency of 0.45 THz, 1 THz, and 2 THz. The R_{res} value for YBCO is obtained from Refs. 13 and 14, in which an 80 nm thick c -axis oriented epitaxial YBCO film was measured by the same technique. The R_s values of MgB_2 at 0.45 THz are almost one order of magnitude lower than the R_{res} of YBCO, and one third of that of YBCO at 2 THz and low temperature (up to 15 K). Figure 3 shows the temperature dependence of R_s at frequencies of 0.45 THz, 1.05 THz, 1.56 THz, and 2.00 THz. The solid lines show the temperature dependence of the surface resistance of copper¹⁶ for comparison. From this figure it is found that R_s for MgB_2 is lower than that of copper below T_c at submillimeter wave and THz frequencies. Such comparisons clearly demonstrate that MgB_2 has advantages over normal metal material and YBCO for THz applications.

In order to compare our measurements with theoretical expectations we use the following model to calculate the complex conductivity: in a two band superconductor like MgB_2 the total conductivity in principle consists of two contributions, one from each band. However, as we have argued earlier,¹⁷ in our films the total conductivity is dominated by the π -band contribution and the contribution from the σ -band can be neglected. We calculate the π -band conductivity $\sigma(\omega)$ from impurity scattering in the Born limit using Eq. (13) in the work of Hensen *et al.*,¹⁸

$$\sigma(\omega) = \sigma_{\text{dc}} \frac{\gamma}{\omega} \int_{-\omega/2}^{\infty} d\Omega \left\{ \left[\tanh \frac{\omega + \Omega}{2k_B T} - \tanh \frac{\Omega}{2k_B T} \right] \times [M_-(\Omega + \omega, \Omega) - M_+(\Omega + \omega, \Omega)] + 2i \tanh \frac{\omega + \Omega}{2k_B T} \text{Im} M_+(\Omega + \omega, \Omega) \right\}, \quad (1)$$

where

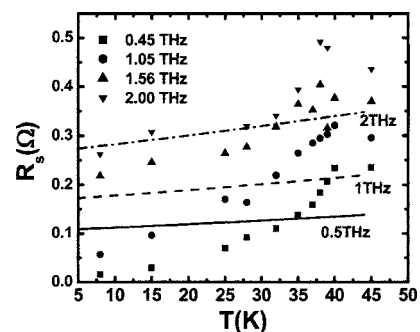


FIG. 3. The temperature dependence of R_s of the MgB_2 thin film at 0.45 THz, 1.05 THz, 1.56 THz, and 2.00 THz. R_s values of copper at 0.5 THz, 1 THz, and 2 THz are also shown as the solid lines for comparison.

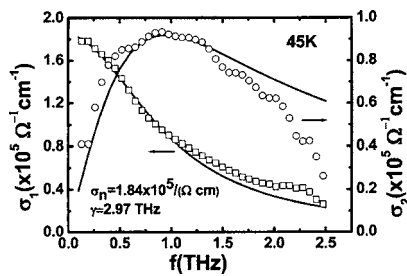


FIG. 4. Frequency dependence of the real part σ_1 (squares) and imaginary part σ_2 (circles) of the complex conductivity at 45 K. The lines show the fit based on the Drude model with the parameters as described in the text. The arrows point to the axis to which the plots correspond.

$M_{\pm}(\Omega + \omega, \Omega)$

$$= \frac{1 + \frac{(\Omega + \omega)\Omega + \Delta^2}{\sqrt{\Delta^2 - (\Omega \pm i0^+)^2} \sqrt{\Delta^2 - (\Omega + \omega + i0^+)^2}}}{2\gamma + \sqrt{\Delta^2 - (\Omega \pm i0^+)^2} + \sqrt{\Delta^2 - (\Omega + \omega + i0^+)^2}}. \quad (2)$$

Here, γ and Δ are the impurity scattering rate and the gap in the π -band, respectively.¹⁸ Equation (2) is equivalent to Eq. (5.9) in the work by Nam¹⁹ and reduces to the Drude model in the normal state. In our calculations we use the values of γ and σ_{dc} from the fit to the normal state data. Figure 4 shows the measured complex conductivity spectra in the normal state (45 K). In the normal state the electrodynamics properties of the MgB₂ thin film can be consistently interpreted in terms of a metallic conductivity. Hence, this frequency behavior should be in accordance with the Drude model, i.e., $\sigma(45K) = \sigma_{dc}/(1 - i\pi f/\gamma)$. Fitting to the experimental data, we obtain $\sigma_{dc} = 1.84 \times 10^5 \Omega^{-1} \text{cm}^{-1}$ and $\gamma = 2.97$ THz. The solid lines represent the fitting result. Compared with other far-infrared and optical measurements on MgB₂ thin films,⁹ the scattering rate in our film is small. This small scattering rate can be attributed to the high-quality of our thin film. For the temperature dependence of the π -band gap Δ we take the temperature dependence from a solution of the two-gap model reported earlier.¹⁷ The complex conductivity was then calculated from Eqs. (1) and (2), and Z_s was derived from it. The results are shown in Figs. 1 and 2 (lines) for the same set of temperatures as in the measurements.

A qualitative agreement could be obtained between calculation and experimental results. R_s obtained from the experiment shows a smooth change around the energy gap, rather than a sharp jump. This is also true for the behavior of X_s —the peak appearing in the calculation could not be observed in the measurement. We suggest that the difference is caused by a low power transmission coefficient T_r of the sample in the THz range and by a smeared density of states at the energy gap. Within the framework of the thin film approximation, we could roughly consider T_r to be proportional to $\lambda^2 \exp(-2t/\lambda)$, where t is the thin film thickness. The high-quality epitaxial thin film has a low λ , which leads to a low T_r , and reduces the signal-to-noise ratio. The singularity of the density of states around the energy gap is smeared, which may be caused by strong electron-phonon coupling effects present in MgB₂ or by the boundary between the nonsuperconducting layer and MgB₂ layer. This

makes it difficult to observe a well defined onset of the gap in Fig. 1.

In conclusion, we carried out THz spectroscopic measurements on an epitaxial thin film with a T_c of 39.1 K and a nominal thickness of 100 nm. At frequencies around 1–2 THz, the film has a lower R_s than both YBCO and copper. We observe a linear dependence of X_s on the frequency, yielding a penetration depth of about 100 nm. The measurements agree qualitatively with calculations, which are based on impurity scattering in the Born limit. The low R_s value demonstrates the great advantage of MgB₂ thin films for passive devices as compared to other superconductors and normal metals due to the higher possible operation temperatures of 20–40 K, which can be achieved by moderate-cost, small-size, low-weight cryocoolers. With respect to recent successful fabrication of all-MgB₂ tunnel junctions,²⁰ it is very promising to develop all MgB₂ THz detectors in the future.

The work at Penn State is supported in part by the ONR under Grant Nos. N00014-00-1-0294 (Xi) and N0014-01-1-0006 (Redwing), and by the NSF under Grant No. DMR-0306746 (Xi and Redwing). F. Kadlec and P. Kuzel are thankful to the Ministry of Education of the Czech Republic for the support (Project No. LC512).

¹M. Tinkham, *Introduction to Superconductivity*, 2nd ed. (McGraw-Hill, New York, 1996).

²A. V. Pronin, M. Dressel, A. Pimenov, A. Loidl, I. V. Roshchin, and L. H. Greene, *Phys. Rev. B* **57**, 14416 (1998).

³M. C. Nuss, P. M. Makiewich, M. L. O'Malley, E. H. Westerwick, and P. B. Littlewood, *Phys. Rev. Lett.* **66**, 3305 (1991).

⁴A. D. Semenov, G. N. Gol'tsman, and R. Sobolewski, *Supercond. Sci. Technol.* **15**, R1 (2002).

⁵J. Nagamatsu, J. N. Nakagawa, T. Muranaka, Y. Zenitani, and J. Akimitsu, *Nature (London)* **410**, 63 (2001).

⁶For a recent review, see T. Dahm, in *Frontiers in Superconducting Materials*, edited by A. V. Narlikar (Springer, Berlin, 2005), p. 983 (cond-mat/410158).

⁷R. A. Kaindl, M. A. Carnahan, J. Orenstein, D. S. Chemla, H. M. Christen, H. Y. Zhai, M. Paranthaman, and D. H. Lowndes, *Phys. Rev. Lett.* **88**, 027003 (2002).

⁸A. V. Pronin, A. Pimenov, A. Loidl, and S. I. Krasnosvobodtsev, *Phys. Rev. Lett.* **87**, 097003 (2001).

⁹J. H. Jung, K. W. Kim, H. J. Lee, M. W. Kim, T. W. Noh, W. N. Kang, Hyeon-Jin Kim, Eun-Mi Choi, C. U. Jung, and Sung-Ik Lee, *Phys. Rev. B* **65**, 052413 (2002).

¹⁰X. H. Zeng, A. V. Pogrebnnyakov, A. Kotcharov, J. E. Jones, X. X. Xi, E. M. Lysczek, J. M. Redwing, S. Y. Xu, Q. Li, J. Lettieri, D. G. Schlom, W. Tian, X. Q. Pan, and Z. K. Liu, *Nat. Mater.* **1**, 35 (2002).

¹¹M. Kempa, P. Kuzel, S. Kamba, P. Samoukhina, J. Petzelt, A. Garg, and Z. H. Barber, *J. Phys.: Condens. Matter* **15**, 8095 (2003).

¹²J. Petzelt, P. Kuzel, I. Rychetsky, A. Pashkin, and T. Ostrapchuk, *Ferroelectrics* **288**, 169 (2003).

¹³I. Wilke, M. Khazan, C. T. Rieck, P. Kuzel, T. Kaiser, C. Jaekel, and H. Kurz, *J. Appl. Phys.* **87**, 2984 (2000).

¹⁴I. Wilke, M. Khazan, C. T. Rieck, P. Kuzel, C. Jaekel, and H. Kurz, *Physica C* **341–348**, 2271 (2000).

¹⁵N. Klein, *Rep. Prog. Phys.* **65**, 1387 (2002).

¹⁶A. N. Luiten, M. E. Tobar, J. Krupka, R. Woode, E. N. Ivanov, and A. G. Mann, *J. Phys. D* **31**, 1383 (1998).

¹⁷B. B. Jin, T. Dahm, A. I. Gubin, Eun-Mi Choi, Hyun Jung Kim, Sung-IK Lee, W. N. Kang, and N. Klein, *Phys. Rev. Lett.* **91**, 127006 (2003).

¹⁸S. Hensen, G. Müller, C. T. Rieck, and K. Schamberg, *Phys. Rev. B* **56**, 6237 (1997).

¹⁹S. B. Nam, *Phys. Rev.* **156**, 470 (1967).

²⁰Hisashi Shimakage, Kazuya Tsojimoto, Zhen Wang, and Masayoshi Tonouchi, *Appl. Phys. Lett.* **86**, 072512 (2005).